Exploring the Crucial Role of Atmospheric Carbonyl Compounds in Regional Ozone heavy Pollution: Insights from Intensive Field Observations and Observation-based modelling in the Chengdu Plain Urban Agglomeration, China

Jiemeng Bao[1,2], Xin Zhang[1,2], Zhenhai Wu[1], Li Zhou[3], Jun Qian[4], Qinwen Tan[5], Fumo Yang[3], Junhui Chen[6], Yunfeng Li[7], Hefan Liu[5], Liqun Deng[6], Hong Li[1*]

[1]Chinese Research Academy of Environmental Sciences, State Key Laboratory of Environmental Benchmarks and Risk Assessment, Beijing 100012, China

[2]School of Environmental Science and Engineering of Peking University, State Key Joint Laboratory of Environmental Simulation and Pollution Control, Joint Laboratory of Regional Pollution Control International Cooperation of the Ministry of Education, Beijing 100871, China

[3]College of Carbon Neutrality Future Technology, Sichuan University, Chengdu 610065, China

[4]Sichuan Radiation Environment Management and Monitoring Central Station, Chengdu 611139, China

[5]Chengdu Academy of Environmental Sciences, Chengdu 610046, China

[6]Sichuan Academy of Eco-Environmental Sciences, Chengdu 610042, China

[7]School of Mechanical Engineering, Beijing Institute of Petrochemical Technology, Beijing 102617，China

Correspondence to: Hong Li (lihong@craes.org.cn)

Abstract. Gaseous carbonyl compounds serve as crucial precursors and intermediates in atmospheric photochemical reactions, significantly contributing to ambient ozone formation. To determine whether the impact of carbonyl compounds on regional ozone pollution is driven by their abundance or by specific secondary chemical processes, simultaneous field observations and observation-based modelling of ambient carbonyls were conducted at nine sites within the Chengdu Plain Urban Agglomeration (CPUA), China during August 4-18, 2019, when three episodes of regional heavy ozone pollution occurred across eight cities within CPUA. Throughout the study, the total mixing ratios of 15 carbonyls ranged from 10.7±4.2 to 35.2±13.4 ppbv. The spatial distribution reveal that regions with higher concentrations of carbonyl compounds, such as around Chengdu, are also areas with more severe ozone pollution. Both the abundance and the

chemical reactivity of carbonyl compounds, especially formaldehyde and acetaldehyde, play crucial roles in ozone formation in the CPUA. On ozone pollution days, carbonyl concentrations significantly increased by 22.8% to 66.2%.While the abundance of carbonyls is an important factor, their significant role in heavy ozone pollution within the CPUA is primarily driven by secondary chemical processes, particularly those involving alkenes and BVOCs. Sites with higher average ozone concentrations during observations were mainly in the VOCs-limited regime, while others were in the transitional regime. Additionally, the mutual transport of carbonyl compounds between cities in the CPUA suggests that regional collaboration is essential to address ozone pollution effectively. These findings offer valuable insights for developing effective strategies to control regional ozone pollution.

Keywords: Gaseous Carbonyls; Ozone Heavy Pollution; Pollution Characteristics; Atmospheric Photochemical Reactivity; Source Analysis; The Chengdu Plain Urban Agglomeration, China

1.   Introduction

Atmospheric carbonyl compounds play a pivotal role in tropospheric chemistry, acting as crucial precursors to both ozone (O_3) and secondary organic aerosols (SOA), a fact recognized for decades (Altshuller, 1993; Grosjean and Seinfeld, 1989). Their importance has been confirmed by numerous studies over the years(Guo et al., 2004; Hallquist et al., 2009; Wang et al., 2020; Ye et al., 2021; Coggon et al., 2019), highlighting their significant contribution to atmospheric photochemistry and air pollution. Over the past two decades, severe air pollution in China has driven substantial research efforts to understand the contributions of carbonyl compounds to these environmental challenges. Studies have shown that photolysis of carbonyl compounds is a major source of RO_X radicals (Grosjean and Seinfeld, 1989; Zhang et al., 2016). These compounds can be photolyzed and react with OH radicals to form a large number of HO_2 and RO_2 radicals, which increase the atmospheric oxidation capacity and participate in the NOx photochemical cycle, leading to ozone formation (Zhang et al.,

2016; Meng et al., 2017). Additionally, dialdehydes such as glyoxal and methylglyoxal undergo heterogeneous reactions with aqueous particulate matter, rapidly forming SOA (Lou et al., 2010; Xue et al., 2016; Yuan et al., 2012). Ambient carbonyl compounds not only affect the environment but also pose direct health risks to humans. They can harm ecosystems through deposition and adsorption processes (Yang et al., 2018). They also pose direct health risks to humans, including sensitization, carcinogenesis, and mutagenicity (Fuchs et al., 2017).

Recent research has increasingly focused on understanding the spatial and temporal variability of carbonyl compounds in highly polluted regions, particularly in China, where rapid industrialization has led to severe air quality challenges. Xue et al. (2013) and Duan et al. (2012) reported typical ambient concentrations of carbonyl compounds ranging from a few $\mu g \cdot m^{-3}$ to tens of $\mu g \cdot m^{-3}$ in urban areas, depending on the specific compounds and regions studied. For example, formaldehyde concentrations in highly polluted areas can exceed 10 $\mu g \cdot m^{-3}$. Shen et al. (2013) and Fu et al. (2008) observed significant diurnal variation, with higher concentrations of carbonyl compounds during the daytime, particularly in the afternoon, driven by photochemical production. Concentrations can increase by as much as 50-100% during peak sunlight hours compared to nighttime levels. Pang and Mu (2006) and Rao et al. (2016) identified key sources of carbonyl compounds, including vehicular emissions, industrial activities, and secondary formation from VOC oxidation in the atmosphere. In urban environments, vehicular emissions are often a dominant primary source, while secondary formation contributes significantly during daytime due to photochemical processes. The results highlight severe and spatiotemporal variations of carbonyl pollution in China. High levels are found mainly in the North China Plain(NCP), the Yangtze River Delta(YRD), and the Pearl River Delta(PRD)(Duan et al., 2008; Shao et al., 2009; Tan et al., 2018; Wang et al., 2018; Xue et al., 2014, 2013; Yang et al., 2017). Urban areas generally exhibit higher carbonyl levels than suburban and rural areas due to human activities(Xue et al., 2013). Despite the progress made, significant gaps

87　remain in understanding the spatiotemporal distribution and source apportionment of

88　carbonyl compounds, particularly in urban agglomerations. Existing research has

89　primarily focused on urban areas in rapidly developing regions like the NCP, YRD, and

90　PRD. Moreover, studies have often emphasized the overall role of VOCs in ozone

91　pollution, with less attention given to specific carbonyl compounds and their individual

92　contributions to atmospheric oxidation capacity and ozone formation (Meng et al.,

93　2017).

94　　Monitoring carbonyl compounds in the atmosphere is challenging due to their

95　typically low concentrations (ppt-ppb levels), necessitating highly sensitive analytical

96　methods. The diversity of carbonyl compounds, including multiple isomers, requires

97　highly selective analytical techniques for differentiation. Current measurement

98　technologies limit our understanding of the spatiotemporal distribution of carbonyl

99　compounds, affecting the accurate assessment of their environmental behavior, sources,

100　and transport (Xue et al., 2013; Sahu and Saxena, 2015). While numerous studies have

101　explored the role of carbonyl compounds in ozone production, many focus on general

102　mechanisms rather than specific compounds or regional variations (Atkinson and Arey,

103　2003; Monks et al., 2015).

104　　Atmospheric carbonyl compounds originate from both primary and secondary

105　sources (Pang and Mu, 2006; Rao et al., 2016). Primary sources include the incomplete

106　combustion of fossil fuels and biomass, industrial emissions, emissions from the

107　catering industry, and releases from plants. Secondary sources arise from the

108　atmospheric photochemical oxidation of VOCs　(Xue et al., 2013), particularly

109　alkenes, aromatics, and isoprene, which typically dominate the secondary formation of

110　carbonyls. However, distinguishing between primary and secondary contributions

111　remains challenging. Existing source apportionment methods, such as characteristic

112　species ratios and multiple linear regression, often lack the resolution to differentiate

113　these sources accurately, especially for non-vehicular emissions and secondary

114　formation. The limitations of these methods underscore the need for more advanced

115 approaches to better quantify the secondary formation mechanisms of carbonyl

116 compounds and their regional impact on ozone formation. Despite significant

117 advancements in studying atmospheric carbonyls, key gaps remain in understanding

118 their precise spatiotemporal distribution and source apportionment. Specifically, there

119 is a need for studies that examine how carbonyls vary across different environments—

120 urban, suburban, and rural—and during varying pollution events. Without such targeted

121 analysis, our understanding of the behavior of carbonyl compounds and their

122 contribution to ozone pollution remains incomplete, particularly in regions

123 experiencing severe pollution.

124   This study focuses on atmospheric carbonyl compounds and their roles in

125 photochemical pollution within the Chengdu Plain Urban Agglomeration (CPUA) of

126 China. The CPUA includes eight cities: Chengdu, Mianyang, Deyang, Leshan, Meishan,

127 Yaan, Suining, and Ziyang. This region has a developed economy and a high degree of

128 internationalization. The CPUA is located on the western edge of the Sichuan Basin,

129 surrounded by mountain ranges, which easily block airflow. The unique climatic

130 environment of the CPUA features low wind speeds year-round, high frequency of

131 static winds, short hours of sunshine, frequent winter inversions, and a pronounced heat

132 island effect in summer. These climatic characteristics significantly impact the

133 variations in air pollutant concentrations, making the region prone to ozone pollution

134 in summer and haze pollution in winter. (Li et al., 2013; Hu et al., 2017; Zhang et al.,

135 2010). Although previous studies have shown that ozone formation in urban Chengdu

136 is primarily VOCs-limited (Tan et al., 2018), with aromatic hydrocarbons and alkenes

137 contributing significantly to ozone generation in summer (Xu et al., 2020), these studies

138 mainly focus on single cities and overall VOCs. There is still limited understanding of

139 whether the significant roles of carbonyl compounds in ozone formation are primarily

140 due to their abundance or whether specific chemical reactions involving carbonyls drive

141 this process. This study aims to address these gaps by investigating the spatial

142 distribution, sources, and specific chemical pathways of carbonyl compounds across

143 the entire CPUA and assessing their contributions to regional ozone pollution and inter-

144 city air transport mechanisms.

145   To address these research gaps, this study involves an intensive field observation

146 experiment conducted by the Sichuan Academy of Environmental Sciences, Peking

147 University, Sichuan University and Chinese Academy of Environmental Sciences.

148 Atmospheric carbonyl compounds were observed at nine sites in eight cities within the

149 CPUA for 15 days during a period of heavy ozone pollution in August 2019. Samples

150 were analyzed using 2,4-dinitrophenylhydrazine solid phase adsorption/high

151 performance liquid chromatography (HPLC). The study aims to characterize the

152 atmospheric carbonyl compounds in the CPUA, assess their influence on

153 photochemical pollution, identify key carbonyl compounds that may play crucial roles

154 in heavy ozone pollution in the CPUA, and evaluate the contribution of primary

155 emissions, air pollution transport, and secondary generation to key carbonyl compounds

156 through a combination of multivariate linear regression modeling and Observation-

157 Based Modeling (OBM). This research aims to provide technical support for controlling

158 carbonyl compounds pollution in the CPUA and to reduce their contributions to ozone

159 pollution.

160 **2. Materials and methods**

161 **2.1 Observation Sites Profile**

162   In this study, a total of 9 off-line sampling sites for atmospheric carbonyl

163 compounds were set up in 8 cities in the CPUA from August 4th to 18th, 2019(table S1).

164 Considering that this study focused on the pollution characterization of carbonyl

165 compounds in urban areas, one urban site was selected in each city. In addition, in order

166 to compare and study the pollution characteristics of carbonyl compounds in the

167 suburbs, a suburban site was set up in Xinjin County, Chengdu. For the selection of

168 urban sites in each city, priority is given to those choices of set-up in the vicinity of the

169 state-controlled site, and the perimeter of the sites should be open, unobstructed and no

170   obvious pollution sources, with convenient transportation and power supply. The

171   distribution of specific sites is shown in Fig. 1.

172   Ozone concentrations were measured using the UV absorption method with a

173   Thermo O_3 analyzer (Model 49i), with data sourced from national control stations near

174   each sampling site. Nitrogen dioxide (NO_2) was measured by chemiluminescence

175   following chemical conversion to nitric oxide (NO) using a molybdenum catalyst;

176   however, this method is known to have interferences from other NO_z species. Carbon

177   monoxide (CO) was measured via infrared absorption with a Thermo instrument

178   (Model 20). All Thermo instruments were carefully maintained and calibrated daily at

179   01:00 to ensure measurement accuracy. Measurements for ozone, NO_2, and CO were

180   collected with a time resolution of one hour. Simultaneously, meteorological

181   parameters—temperature, relative humidity (RH), wind speed, and direction—were

182   recorded at each observation site using an automatic weather station (PC-4, JZYG,

183   China), also at a one-hour resolution.
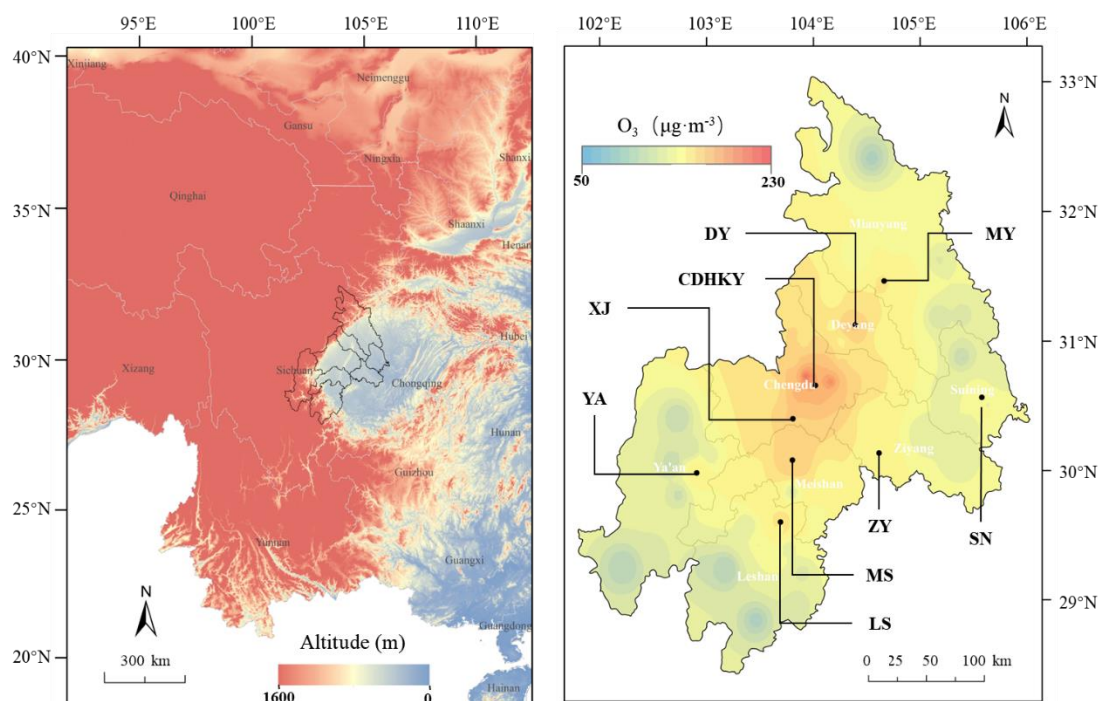
184

185   **Figure 1.** Distribution of sampling sites. The left panel shows the elevation map of the Sichuan

186   Basin, highlighting the geographical features of the region, with elevation data sourced from the

187   Geospatial Data Cloud (https://www.gscloud.cn/#page1/2). The right panel presents the spatial

188   distribution of ozone concentrations in the CPUA during the observation period (August 4–18,

7

189   2019), with ozone data obtained from national control stations near each sampling site. Black dots
190   represent the locations of the sampling sites, labeled as follows: MY (Mianyang), DY (Deyang),
191   CDHKY (Chengdu Environmental Science Research Institute), XJ (Xinjin), SN (Suining), ZY
192   (Ziyang), MS (Meishan), YA (Ya'an), and LS (Leshan). The color bar in the top left corner
193   corresponds to interpolated ozone concentrations, with each color representing a concentration
194   gradient.

195   **2.2 Samples Collection**

196   The sampling of atmospheric carbonyl compounds mainly referred to the TO-11A

197   standard of the United States Environmental Protection Agency (US EPA) and the

198   Chinese environmental protection standard HJ 683-2014 High Performance Liquid

199   Chromatography Method for the Determination of Atmospheric Carbonyl Compounds,

200   and the sampling was carried out by using silica gel sampling tubes (IC-DN3501 from

201   Tianjin Bonna-Agela) coated with DNPH (2,4-dinitrophenylhydrazine). In this study,

202   an automatic sampler for carbonyl compounds (Zhang et al., 2019) was used to

203   continuously collect atmospheric carbonyl compounds. From August 4th to 18th, 2019,

204   air samples were collected every 2 hours with a sampling flow rate of 0.8 L·min^{-1}. In

205   addition, in order to prevent the impact of ozone and rainwater in the atmospheric air

206   on sample collection, a potassium iodide ozone removal column (KI 140 from Tianjin

207   Bonna-Agela) was installed and a water removal agent made by ourselves (Bao et al.,

208   2022; Wang et al., 2020) was added at the front end of the sample tube. Two blank

209   samples were collected before and after the sampling, and blank samples were also

210   collected for different batches of sampling tubes. The samples were frozen at -18°C and

211   analyzed within one month.

212   Atmospheric VOCs were sampled using SUMMA tanks, stainless steel tanks with

213   electropolished and silanized inner walls, manufactured by Entech in the United States,

214   with a sampling volume of 3.2 liters. The sampling was controlled by a constant current

215   integral sampler to sampling for an average of 1 hour. From August 4th to 18th, 2019,

216   two VOCs samples were collected each day at each site, at 8:00-9:00 and 14:00-15:00

217   (no samples were taken under special weather conditions, such as rain). On August 11th,

218   12th and 16th , six samples were collected per day to capture diurnal variations under

219   ozone pollution events, at the following times: 8:00-9:00, 10:00-11:00, 12:00-13:00,

220   14:00-15:00, 16:00-17:00, and 18:00-19:00.

221   **2.3 Samples Analysis**

222   The carbonyl compounds samples were qualitatively and quantitatively analyzed

223   by using High Performance Liquid Chromatography (HPLC) (LC-20AD, Shimadzu,

224   Japan) and an ultraviolet detector (SPD-20A, Shimadzu, Japan), mainly based on the

225   US EPA TO-11A standard and the Chinese HJ 683-2014 standard. The DNPH sampling

226   column after sampling was slowly eluted into a volumetric flask using acetonitrile

227   (chromatographically pure, Thermo Fisher Scientific China) to 5.0 mL. Then 1.5 mL of

228   the sample was transferred into an HPLC sample bottle, and sealed and stored in a

229   refrigerator at <4 ℃ to complete the pre-treatment. Prior to sample analysis, a standard

230   solution of the concentration gradient was prepared using TO-11A standard solution

231   (Supelco, USA) and used as the external standard. The correlation coefficient (R^2) of

232   the standard curve was greater than 0.995. The detection limit of the device was

233   0.56~5.57 ng·mL^{-1}, and the quantification limit was 1.87~18.56 ng·mL^{-1} (Table S2).

234   Then 20 μL of the pretreated sample was extracted through the autosampler and injected

235   into the HPLC/UV system, detected by a UV detector with a wavelength of 360 nm,

236   qualified by retention time value, quantified by peak area value, and the qualitative and

237   quantitative analysis data of carbonyl compounds were obtained after conversion. The

238   HPLC conditions referred to Chinese environmental protection standard HJ 683-2014:

239   binary gradient washing was performed using acetonitrile and water, 60% acetonitrile

240   was held for 20 mins, acetonitrile was increased linearly from 60% to 100% within 20-

241   30 mins, and acetonitrile was reduced to 60% again within 30-32 mins and held for 8

242   mins; the column oven was kept at 40 ℃. It should be noted that while the sampling

243   and analysis method was effective for most carbonyl compounds, ketones, including

244   methyl vinyl ketone (MVK), were not well sampled during the field observations. As a

245   result, data for MVK and other ketones were missing. During the observation period,

246   DNPH cartridges and HPLC analysis technique were used to detect a total of 15

247   carbonyl compounds (Table S2).

248   The atmospheric VOCs were analyzed using the TO-14 and TO-15 methods,

249   which are recommended by the US EPA. These methods involve frozen

250   preconcentration coupled with gas chromatography and mass spectrometry (GC-MS).

251   TO-15 is a method for detecting and quantifying a wide range of VOCs from air samples.

252   The VOCs were pre-concentrated by the Entech7100 system at a low temperature, then

253   quantified by an Agilent GC-MS. During the sample analysis, four internal standard

254   gases (bromochloromethane, 1,4-difluorobenzene, chlorobenzene-d5, and 4-

255   bromofluorobenzene) were used. A multi-point calibration curve was created using a

256   standard gas containing 118 VOCs, including PAMS compounds, TO-15 target analytes,

257   and carbonyl compounds. PAMS (Photochemical Assessment Monitoring Stations)

258   compounds are a subset of hydrocarbons known to contribute to ozone formation, such

259   as ethane, ethylene, propane, and others.

260   **2.4 Data Analysis**

261   **2.4.1 Ozone pollution assessment criteria**

262   According to the Technical Regulation on Ambient Air Quality Index (on trial),

263   National Environmental Protection Standard of the People's Republic of China HJ

264   633—2012, days with an ozone pollution index (IAQI) of 100 or higher during the

265   observation period were designated as pollution days, while days with an IAQI below

266   100 were considered clean days. This study compared the pollution characteristics of

267   carbonyl compounds between pollution days and clean days. Additionally, the

268   concentrations of formaldehyde, acetaldehyde, and acetone observed during the

269   summer of 2009-2013 in economically developed and industrialized areas such as

270   Beijing, Shanghai, and Guangzhou in China, as well as locations in South America

271   (Brazil), Asia (Thailand), Europe (France), and North America (United States), were

272   selected and compared.

273   **2.4.2 Ozone formation sensitivity**

274   Previous studies have shown that the formaldehyde to NO_2 ratio (FNR) can be

275 used to determine the sensitivity of O_3-NOx-VOCs (Schroeder et al., 2017; Tonnesen

276 and Dennis, 2000; Vermeuel et al., 2019). Most studies used satellite remote sensing-

277 based FNR, but the FNR column concentration ratios inverted by satellite remote

278 sensing mainly represented the average photochemical of the troposphere, and the

279 concentration distributions of HCHO and NO_2 in the vertical direction were

280 inconsistent (Hong et al., 2022; Schroeder et al., 2017). So, there is a large uncertainty

281 to develop ground-level ozone pollution prevention and control measures. In this study,

282 sensitivity analysis of ground-level ozone formation was carried out based on the ratio

283 of ground-level HCHO to NO_2 during the observation period at the 9 sites of 8 cities in

284 the CPUA. FNR < 0.55±0.16 and FNR > 1.0±0.3 were defined to VOCs-limited and

285 NOx-limited, respectively, and FNR ratio ranged from 0.55±0.16 to 1.0±0.3 defined to

286 NO_X and VOCs co-limited (Liu et al., 2021; Zhang et al., 2022).

287 **2.4.3 Exploration of Secondary Formation Mechanisms**

288 **(1) Atmospheric chemical reactivity**

289   In this study, the contribution of atmospheric chemical reactivity of carbonyl

290 compounds to ozone formation was evaluated using the OH free radical consumption

291 rate (L_{OH}) and ozone formation potential (OFP):

292 $$L_{OH} = [OVOC]_i \times k_i(OH) \tag{1}$$

293   Where, $[OVOC]_i$ was the observed concentration of the ith (i=1 to n) carbonyl

294 compound, in molecule·cm^{-3}; $k_i(OH)$ was the rate constants of the ith carbonyl

295 compound reacting with OH radicals, in cm^3·(molecule·s)$^{-1}$. The unit of L_{OH} is s^{-1},

296 representing the rate of OH radical consumption. The selected $k_i(OH)$ values were from

297 literature (Atkinson and Arey, 2003).

298 $$OFP = MIR_i \times [OVOC]_i \tag{2}$$

299   Where, MIR was the maximum incremental reactivity of the ith carbonyl

300 compound，in g O_3·(g VOC)$^{-1}$ (grams of ozone formed per gram of volatile organic

301   compound), and the MIR values of each species were from California Code of

302   Regulations (https://govt.westlaw.com); [OVOC]$_i$ was the mass concentration of the ith

303   carbonyl compound, in $\mu g \cdot m^{-3}$. The unit of OFP is $\mu g \cdot m^{-3}$, representing the potential

304   ozone formation.

305   **(2) Observation-based model (OBM)**

306   The Observation-Based Model (OBM) is a box model that uses actual

307   observational data to evaluate the sensitivity of secondary pollutant formation

308   mechanisms to their precursor emissions. By constraining the model with atmospheric

309   observation data, typical secondary pollutants and parameters such as NO_X, SO_2, CO,

310   VOCs, temperature, humidity, pressure, and JNO_2 are input into the model as hourly

311   observational data to calculate the chemical formation and consumption of secondary

312   pollutants and free radicals. In this study, the OBM model used the Master Chemical

313   Mechanism (MCM) (v3.3.1, mcm.leeds.ac.uk), which is a nearly detailed chemical

314   mechanism that describes the chemical processes of 143 VOC species from emission

315   to degradation in the atmosphere, including approximately 6,700 species and 17,000

316   inorganic and organic reactions. In this version of the MCM, a total of 19 carbonyl

317   compounds are included, comprising 9 aldehydes and 10 ketones. Of these, 9 carbonyl

318   compounds were measured in this study, including formaldehyde, acetaldehyde,

319   acetone, propionaldehyde, crotonaldehyde, butyraldehyde, isovaleraldehyde,

320   valeraldehyde, and hexaldehyde. The MCM chemical mechanism can simulate

321   atmospheric photochemical reaction processes under near-real conditions and calculate

322   the concentrations of highly reactive species, quantifying the reaction rates of all

323   species involved. For VOCs, especially carbonyls, that were not directly measured, the

324   MCM uses estimated values derived from emission inventories, literature data, and

325   assumptions based on similar species to provide estimates for their concentrations and

326   reaction rates.

327   Relative Incremental Reactivity (RIR) was first used by Cardelino and Chameides

328 (1995) to simulate the response of ozone to precursor changes through scenario tests

329 using box model calculations. RIR was calculated by assuming that the concentration

330 of a given carbonyl compound precursor decreased by a certain proportion could cause

331 the change of the concentration of the carbonyl compound, so as to further judge the

332 effect of VOCs on the formation of carbonyl compounds. Combining the concentrations

333 and activity levels of 15 carbonyl compounds during the observation period, this study

334 focused on formaldehyde, acetaldehyde, and acetone as the primary research targets.

335 The impacts of various AVOCs（anthropogenic VOCs）,including alkanes, alkenes,

336 alkynes, and aromatic hydrocarbons, as well as BVOCs（biogenic VOCs）like isoprene,

337 on the formation of formaldehyde, acetaldehyde, and acetone were assessed using

338 observation-based OBM classification. Specific species of anthropogenic source VOCs

339 (alkanes, alkenes, alkynes, and aromatic hydrocarbons) and biogenic VOCs (isoprene)

340 are detailed in Table S3.

341   VOCs observations, conventional gases (NO_2, CO and SO_2) and meteorological

342 parameters (temperature, relative humidity and pressure) were imputed into the model.

343 It was assumed that the pollutants are well mixed. Under the constraints of the measured

344 hourly concentration data of pollutants, the atmospheric chemical process was

345 simulated to obtain the source-effect relationship of the measured pollutants. By

346 assuming the reduction of the source effect, the RIRs of different carbonyl compounds

347 precursors were calculated, and the sensitivities of carbonyl compounds to different

348 pollutants were obtained, and then the secondary formation mechanism of carbonyl

349 compounds was determined. The formula to calculate the RIR is as follows:

350
$$RIR(X) = \left[\frac{\Delta P_Y(X)/P_Y(X)}{\Delta S(X)/S(X)}\right] \tag{3}$$

351
$$P_Y = Y_{\text{net formation}} - Y_{\text{net consumption}} \tag{4}$$

352   Where X was a specific species; $P_Y(X)$ was the net formation rate of species y;

353 S(X) was the total amount of emissions of species X in a certain period, i.e., the source

354 effect of species X. $\Delta S(X)$ was the change in total emissions of X caused by the

355 hypothetical change in source effect, $\Delta P_Y(X)$ was the change in $P_Y(X)$ after the change

356 in source effect S(X), and RIR(X) was the relative incremental reactivity of species X.

357 The species Y in this study were formaldehyde, acetaldehyde and acetone, respectively,

358 and pollutant X was reduced by 20%.

359   The absolute RIR of the precursor reflects the sensitivity of carbonyl compounds

360 formation to the precursor. The higher the absolute RIR, the more sensitive the carbonyl

361 compounds formation to the precursor. A positive RIR value indicates that reducing the

362 species can reduce the formation rate of species Y, and a negative RIR value indicates

363 that reducing the species can increase the formation rate of species Y.

364 **2.4.4 Sources Analysis**

365 **(1) Multi-linear regression model**

366   There is a good correlation between concentrations of compounds of the same or

367 similar source in the atmosphere. Based on this property, it was assumed that the

368 primary and secondary sources of carbonyl compounds were linearly correlated with

369 the selected tracers, and then a quantitative source model was established by multiple

370 linear statistical regression analysis (Kanjanasiranont et al., 2016a; Li et al., 2010; Ling

371 et al., 2017; Luecken et al., 2012; Lui et al., 2017; Wang et al., 2017). In general, CO is

372 the marker product of typical anthropogenic combustion source emissions, mainly from

373 vehicle exhaust emissions and coal combustion. Ozone, as an indicator of

374 photochemical smog, is a typical secondary formation pollutant. In this study, CO and

375 ozone were selected as the tracers of primary source and secondary source of carbonyl

376 compounds, respectively. The formula is as follows:

377
$$[carbonyl] = \beta_0 + \beta_1[CO] + \beta_2[O_3] \qquad (6)$$

378   Where [carbonyl], [CO] and [O_3] represented the observed mixing ratios of

379 carbonyl compounds, CO and ozone, respectively, in ppbv. β_0, β_1 and β_2 were

380 coefficients obtained by multiple linear regression fitting model, in ppbv/ppbv. β_0

381 represented the background concentration of a given carbonyl compound, β_1

382 represented the emission ratio of the carbonyl compound relative to CO. $\beta_1[CO]$ and

383 $\beta_2[O_3]$ represented the concentrations of carbonyl compound in primary emission and

384 secondary formation, respectively, in ppbv.

385   In addition, the relative contribution of primary emissions, secondary formation

386 and background concentrations of carbonyl compounds can be calculated using the

387 following formula:

388
$$P_{primary} = \frac{\beta_1[CO]_i}{(\beta_0 + \beta_1[CO]_i + \beta_2[O_3]_i)} \times 100\% \qquad (7)$$

389
$$P_{secondary} = \frac{\beta_2[O_3]_i}{(\beta_0 + \beta_1[CO]_i + \beta_2[O_3]_i)} \times 100\% \qquad (8)$$

390
$$P_{background} = \frac{\beta_0}{(\beta_0 + \beta_1[CO]_i + \beta_2[O_3]_i)} \times 100\% \qquad (9)$$

391   Where, $P_{primary}$ represented the contribution of the primary emission of a given

392 carbonyl compound, %; $P_{secondary}$ represented the contribution of the secondary

393 formation of the carbonyl compound species, %; $P_{background}$ represented the contribution

394 of the carbonyl compounds species from sources other than primary emissions and

395 secondary formation, %.

396 **(2) Backward trajectory model**

397   The effects of long-distance air mass transport on the pollution of carbonyl

398 compounds in the CPUA were studied using MeteoInfo software and TrajStat plug-in

399 （http://www.meteothink.org/downloads/index.html）.In this model, meteorological

400 data were relevant meteorological data from the global date assimilation system (GDAS)

401 database (ftp://arlftp.arlhq.noaa.gov/pub/archives/gdasl). A trajectory simulation height

402 of 500 m above ground level (AGL) was selected. The duration of backward trajectory

403 was 48 h. The daily start time was 00:00 UTC. The analog frequency was 2 h. The

404 backward trajectory diagram was calculated. Meanwhile, the clustering method in

405 TrajStat software and the Euclidean distance algorithm were used to cluster the airflow

406 trajectory to the CPUA. And then the statistical analysis was carried out in combination

407 with the corresponding pollutant mass concentration characteristics.

408 **3. Results and Discussion**

3.1 Overview of air quality during observation period

Due to the influence of cooling and precipitation caused by cold air intrusion, the early observation period (from August 4th to 6th, 2019) in the Chengdu Plain Urban Agglomeration (CPUA) experienced slightly lower temperatures (25.1°C) and higher humidity (87.6%). These conditions were unfavorable for ozone formation. Although ozone itself is not easily removed by rain, precipitation reduces ozone pollution by washing away its precursors, such as nitrogen oxides (NOx) and polar volatile organic compounds (VOCs), such as aldehydes, ketones, and others, decreasing sunlight exposure, and enhancing atmospheric dispersion. However, as temperatures increased and humidity dropped in the subsequent days, more favorable conditions for ozone formation emerged, leading to heavy and persistent regional ozone pollution in the CPUA. By August 12th, the mean temperature had gradually increased to 29.1°C, while it averaged 27.7°C from August 13th to 14th. During this time, cumulative precipitation reached 975 mm, resulting in temporary alleviation of ozone pollution. Subsequently, temperatures rose again from August 15th to 18th, with the mean temperature persisting above 28.4°C for several days, accompanied by a decrease in humidity to a minimum of 64.8% on August 17th. Overall, during the observation period (from August 4th, 2019, 0:00 to August 18th, 2019, 24:00), three episodes of severe ozone pollution occurred, namely EP1 (August 7th to 9th), EP2 (August 10th to 13th), and EP3 (August 15th to 18th), as depicted in Fig. 2.

Fig.3 illustrates the temporal and spatial variations of ozone and NO_2 concentrations, as well as temperature and humidity at each site during the observation period. After observing the spatial distribution of ozone concentration during EP1, it's evident that the severity of pollution reached heavily polluted levels, with Chengdu recording an MDA8 concentration of 297 $\mu g \cdot m^{-3}$ on August 7th. This distribution demonstrated a radial decrease from Chengdu to the surrounding areas. However, the subsequent episodes, EP2 and EP3, exhibited even broader ranges of ozone pollution and more pronounced spatial movements. During the early stages of EP2 and EP3 (from

437   August 10th to 11th and from August 14th to 15th, respectively), high ozone

438   concentrations were observed in the Chengdu-Deyang-Mianyang region. In the middle

439   stages (August 12th and from August 16th to 17th, respectively), influenced by northerly

440   airflow, regions with high ozone concentrations expanded to the central (Meishan,

441   Ziyang, and Suining) and southwestern (Leshan and Ya'an) parts of the CPUA. In the

442   later stages (August 13th and August 18th), under the influence of northwesterly airflow,

443   regions with high ozone concentrations (Meishan and Leshan) moved southward again,

444   while ozone pollution in other areas of the CPUA gradually weakened. On August 11th

445   to 12th and August 16th to 17th, ozone concentrations in the eight cities of the CPUA

446   reached light pollution levels or higher, with the heaviest pollution recorded on August

447   12th. Specifically, Deyang, Mianyang, Suining, and Meishan reached moderate

448   pollution levels, while Chengdu reached heavy pollution with a concentration of 324

449     $\mu g \cdot m^{-3}$.

450
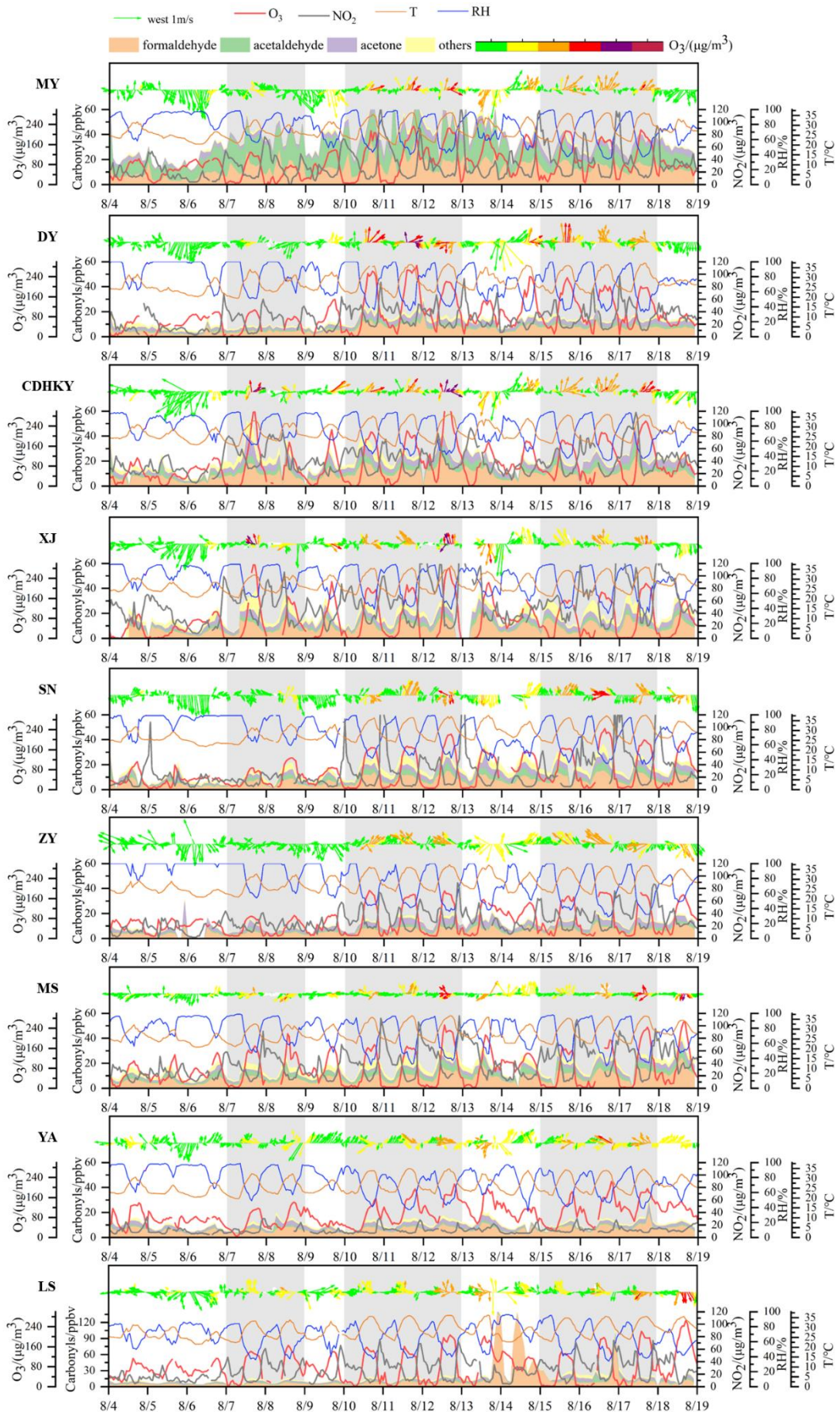
Figure 2. Overview of air quality at each site during the observation period. The gray shaded parts

452   respectively represent the three heavy ozone pollution episodes (EP1, EP2,EP3).
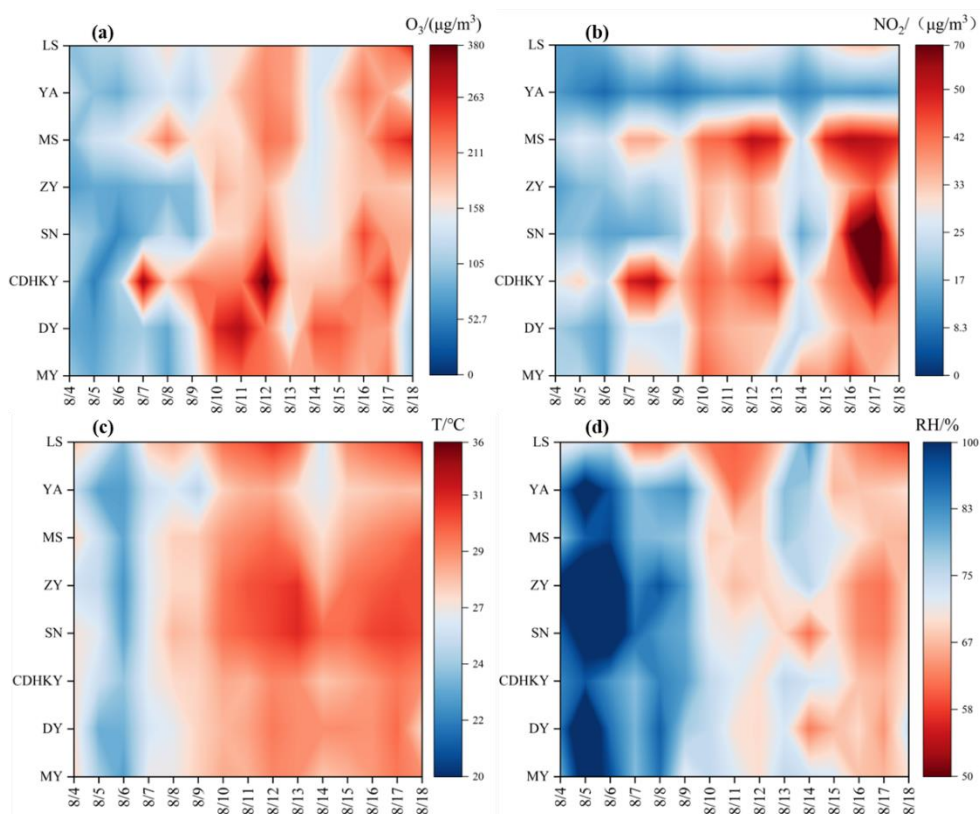
453

454 **Figure 3.** Temporal and spatial variations of (a) ozone concentration, (b) NO$_2$ concentration, (c)

455   temperature and (d) humidity in the CPUA during the observation period.

456 **3.2 Comparative characterization of carbonyl compounds**

457 **3.2.1 Ambient levels**

458   During the observation period, we utilized 2,4dinitrophenylhydrazine (DNPH)

459 cartridge and high-performance liquid chromatography (HPLC) analysis technique to

460 quantify 15 carbonyl compounds. The concentrations and relative proportions of these

461 compounds are summarized in Table 1. The average total concentration of the 15

462 carbonyls in the CPUA was 17.4 ± 5.3 ppb. Overall, areas with elevated concentrations

463 of carbonyl compounds were primarily concentrated in and around Chengdu in both

464 northern and southern directions. MY site, located to the north of Chengdu, exhibited

465 the highest concentration of carbonyl compounds (35.2 ± 13.4 ppb), while YA site,

466 situated southwest of Chengdu, showed the lowest concentration (10.7 ± 4.2 ppb).

467

468   **Table 1.** Daily mean ± standard error of carbonyl compound mixing ratios (ppbv) at each site in

469   the CPUA during the observation period. Sum: the total sum of carbonyl compound mixing ratios

470   across all compounds at each site.

Carbonyls	MY	DY	CDHKY	XJ	SN	ZY	MS	YA	LS
formaldehyde	12.8±6.5	6.1±2.8	10.1±4.2	8.9±4.4	7.0±3.6	5.8±2.7	8.5±4.2	6.4±2.4	6.6±3.4
acetaldehyde	16.7±7.4	1.5±0.8	3.7±2.2	2.3±1.1	2.6±1.7	1.4±0.6	3.2±1.6	0.9±0.7	1.6±1.3
acetone	4.4±1.7	2.8±1.2	4.5±2.3	3.7±1.2	3.1±1.7	3.2±1.7	2.2±1.1	2.2±1.1	2.9±1.6
propionaldehyde	0.4±0.2	0.2±0.1	0.4±0.3	0.4±0.2	0.3±0.2	0.3±0.1	0.4±0.2	0.2±0.12	0.3±0.2
crotoraldehyde	0.2±0.2	0.1±0.1	0.2±0.3	0.1±0.1	0.2±0.1	0.2±0.3	0.2±0.2	0.4±0.2	0.1±0.2
butyaldehyde	0.2±0.5	0.2±0.3	0.4±0.6	0.9±1.7	0.3±0.2	0.1±0.2	0.4±0.5	0.3±0.2	0.0±0.1
benzaldehyde	0.0±0.0	0.0±0.1	0.0±0.1	0.2±0.2	0.1±0.1	0.0±0.0	0.0±0.0	0.0±0.0	0.0±0.0
isovaleraldehyde	0.0±0.1	0.0±0.1	0.1±0.1	0.1±0.1	0.1±0.1	0.0±0.1	0.7±0.4	0.0±0.1	0.1±0.1
valeraldehyde	0.0±0.0	0.3±0.1	0.3±0.6	0.6±0.4	0.9±0.7	0.0±0.0	0.0±0.0	0.0±0.0	0.8±0.5
o-Tolualdehyde	0.5±0.5	0.4±0.3	0.5±0.2	0.0±0.0	0.0±0.0	0.2±0.2	0.4±0.3	0.2±0.2	0.2±0.2
m-Tolualdehyde	0.0±0.0	0.0±0.1	0.0±0.1	0.2±0.2	0.3±0.1	0.0±0.0	0.0±0.0	0.0±0.0	0.0±0.1
p-Tolualdehyde	0.0±0.0	0.0±0.1	0.0±0.0	0.0±0.0	0.0±0.0	0.0±0.0	0.0±0.0	0.0±0.0	0.0±0.0
hexaldehyde	0.0±0.0	0.3±0.3	0.4±0.7	0.6±0.5	1.0±0.7	0.0±0.2	0.8±0.6	0.0±0.0	0.1±0.3
2,5-diemthybenzaldehyde	0.0±0.0	0.0±0.0	0.0±0.0	0.1±0.1	0.0±0.0	0.0±0.0	0.0±0.0	0.0±0.0	0.0±0.0
MACR	0.0±0.2	0.1±0.2	0.3±0.3	1.1±1.1	0.3±0.2	0.2±0.2	0.4±0.4	0.2±0.2	0.8±0.9
Sum	35.2±13.4	12.2±4.8	20.8±8.9	19.0±8.1	16.1±7.7	11.5±4.9	17.2±7.6	10.7±4.2	13.5±6.1

471

472

473

474   Fig.S1 illustrates the relationship between ozone concentration and carbonyl

475   compounds concentration at each site during the observation period. It is evident that

476   the spatial distribution of carbonyl compound concentrations is similar to that of ozone

477   concentration. Regions with severe ozone pollution tend to exhibit higher

478   concentrations of carbonyl compounds. The variation in carbonyl compound

479   concentrations is primarily attributed to anthropogenic emissions and prevailing

480   summer wind directions in the CPUA. Chengdu is the most economically developed

481   city in the CPUA, with notably higher GDP and industrial production values than other

482   regions. Chengdu's major industries include coal-fired power plants, chemical plants,

483   metallurgy and building materials plants, and high concentrations of carbonyls were

484   observed in here. The unique basin climate of the CPUA, characterized by intense

485   sunlight and stable atmospheric conditions, facilitates the accumulation of pollutants.

486   Large amount of industrial emissions and strong photochemical reaction contributes to

487   ozone pollution. Additionally, during the summer, prevailing northerly winds in the

488   CPUA facilitate the downwind transport of pollutants from upwind sources, leading to

489   regional pollution. It is noteworthy that the concentration of carbonyl compounds at the

490   MY site significantly exceeds that at the CDHKY site. Mianyang, with its industrial

491   roots, consistently maintains its position as the second-highest GDP contributor in

492   Sichuan Province. The electronics information industry stands as Mianyang's primary

493   economic driver, constituting approximately half of the city's total output value. Studies

494   investigating the volatile organic compound (VOC) source profile in Chengdu(Zhou et

495   al., 2021) reveal that ethanol and carbonyls predominantly characterize electronics

496   manufacturing emissions.

497   **3.2.2 Compositional characteristics**

498   According to the composition characteristics of 15 carbonyl compounds in the

499   ambient air of each city during the observation period（Table S4）.Formaldehyde was

the most abundant carbonyl found in these sites followed by acetone and acetaldehyde, which is widely observed in previous studies. The measured ratios of formaldehyde, acetone, and acetaldehyde across different sites ranged from 36.4% to 59.4% (average 48.1%), 12.4% to 28.1% (average 19.9%), and 8.2% to 47.3% (average 17.5%), respectively. In this study, the total measured of formaldehyde, acetaldehyde, and acetone（FAT）account for over 78% of the total carbonyls concentrations. At the MY and ZY sites, this proportion even exceeded 90%. It is noteworthy that isobutyraldehyde (MACR) ranks fourth in the volume concentration of 15 carbonyls measured in the ambient air surrounding XJ, accounting for 5.3%. MACR, a characteristic product of isoprene photooxidation from biogenic sources, possibly originates from the abundant vegetation surrounding XJ. It reflects the period's relatively active photochemical reactions, with substantial contributions from secondary formation to the measured carbonyls composition.

The observed levels of FAT in different areas were influenced by various factors including sampling period, geographic location, meteorological conditions, chemical removal, and source emissions(Z. Zhang et al., 2016). Despite these influences, comparisons remain valuable in providing an overview of ambient carbonyl levels in the CPUA. During the summer of 2010, a national wide survey of ambient monocarbonyl compounds were conducted simultaneously in nine sites (Ho et al., 2015)found that the total FAT concentration was highest in Chengdu (14.96 ppb), followed by Beijing (11.83 ppb), and Wuhan (11.70 ppb). Beijing, as the capital of China, and Wuhan, being one of the top ten most populous cities in China, played significant roles in this comparison. In our study, the CDHKY site within CPUA exhibited the highest FAT concentration, with values of 18.25 ppb, surpassing those recorded in 2010. Furthermore, the total FAT concentrations observed at the CPUA and XJ sites, with values of 14.99 ppb and 14.90 ppb respectively in our study, closely resemble those reported in August 2010 in Chengdu. The consistently high levels of carbonyl compounds observed in Chengdu, both in 2010 and our current study, indicate

528 that the city likely experiences higher concentrations of these pollutants compared to

529 other regions across the country. However, more extensive temporal data would be

530 beneficial to fully validate this pattern at a national scale. Comparing our findings to

531 international studies, the FAT concentrations at the CDHKY site were lower than those

532 reported in Rio De Janeiro, Brazil(da Silva et al., 2016), during July to October 2013

533 (35.43 ppb), but higher than those in Bangkok, Thailand(Kanjanasiranont et al., 2016b),

534 Orleans, France(Jiang et al., 2016), and the United States(Murillo et al., 2012), with

535 values of 9.05 ppb, 6.12 ppb, and 5.76 ppb, respectively.

536 **3.3 Temporal variations of carbonyl compounds**

537 The diurnal variation of the total mixing ratio of ambient carbonyl compounds and

538 ozone concentration around each site in the CPUA during the observation period is

539 shown in Fig. 4. According to the observation results, the diurnal trend of ozone

540 concentration at each site showed a "unimodal" variation characteristic, that was, it

541 gradually increased from the morning to the peak of one day at noon, and then decreased.

542 The diurnal variation of the total mixing ratio of carbonyl compounds at each site

543 generally showed a characteristic of high during the daytime and low at night. The

544 concentration of carbonyl compounds during the day (6:00-16:00) was 48.8% higher

545 than that at night (18:00-4:00) at the XJ site. This indicated that the concentration of

546 carbonyl compounds increased by photochemical production during the daytime.

547 Additionally, deposition processes, particularly dry deposition at night, likely

548 contribute to the observed diurnal variation in carbonyl levels. The diurnal variation

549 characteristics of each site were different. For example, the diurnal variation

550 characteristics of carbonyl compounds concentration at CDHKY, XJ and SN sites were

551 consistent with those of ozone. The diurnal variation of carbonyl compounds

552 concentrations at other sites showed "double peaks", peaking at 10:00-12:00 and 18:00-

553 20:00, respectively. The concentrations of carbonyl compounds at night were also

554 higher at MY, DY and LS sites. The diurnal minimum values of the total concentration

555 of carbonyl compounds and ozone concentration appeared at similar time, usually at

556 4:00 a.m. or 6:00 a.m. The first peak of the total mixing ratio of carbonyl compounds

557 occurred earlier than the maximum ozone concentration of the day. The first peak of

558 the total mixing ratio of carbonyl compounds mostly occurred between 10:00 and 12:00.

559 And the maximum ozone concentration mostly occurs between 14:00 and 16:00. This

560 was related to the fact that carbonyl compounds were important precursors of ozone.

561   In general, the diurnal variation of the total concentration of carbonyl

562 compounds on pollution days and clean days was high during the daytime and low at

563 night. The total mixing ratio of carbonyl compounds on pollution days was 22.8%-

564 66.2% higher than that on clean days. At the same time, the increase of concentration

565 of carbonyl compounds during the daytime on pollution days was higher than that on

566 clean days. This suggested that the increase in the concentration of carbonyl

567 compounds during the daytime contributed to ozone pollution.
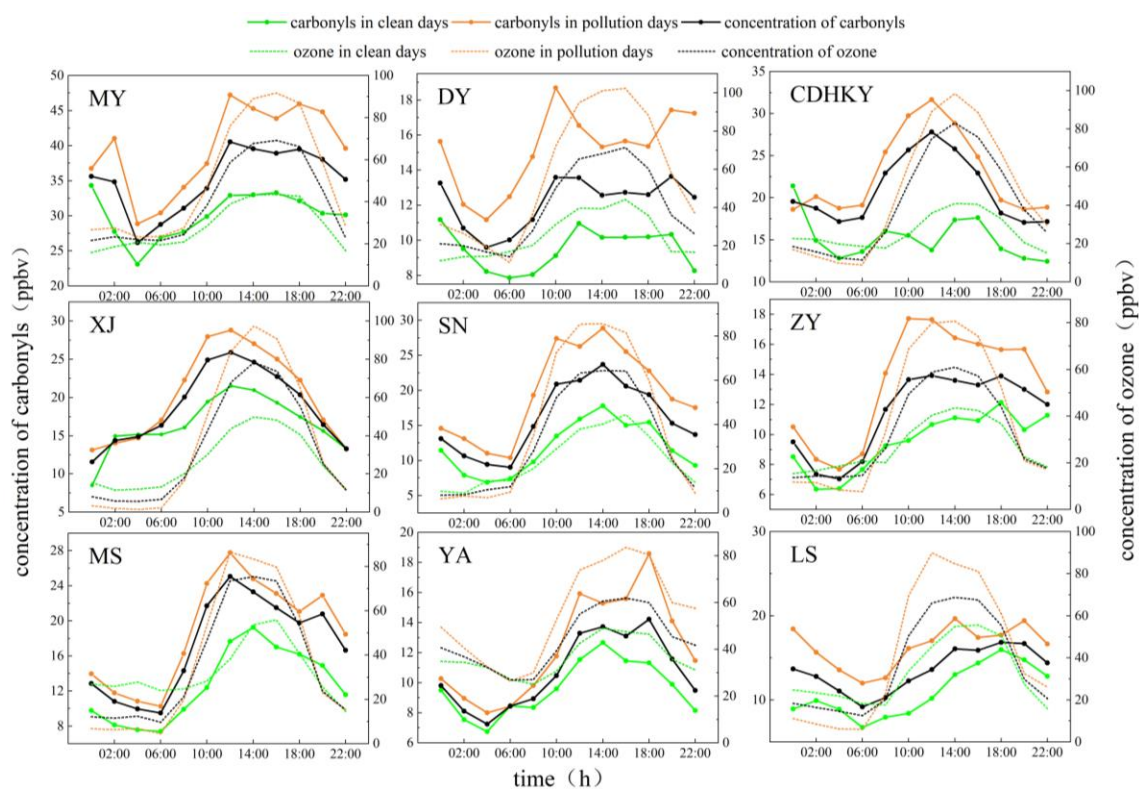
569 **Figure 4.** Diurnal variations of carbonyl compounds and ozone concentrations at each site in the

570   CPUA during the observation period

571 **3.4 Atmospheric photochemical reactivity of carbonyl compounds**

572   During the observation period, the total OH radical consumption rate (L_{OH}) and

total ozone formation potential (OFP) of the 15 carbonyl compounds at each site are depicted in Fig.5. The ranking of total L_{OH} and total OFP at each site is consistent, except for the YA and ZY sites with lower concentrations of carbonyl compounds, where the atmospheric photochemical reactivity ranking also aligns with the concentration. Among all sites, the MY and CD sites display the highest reactivity, while the YA and ZY sites exhibit the lowest reactivity. During the observation period, carbonyl compounds significantly contributed to ozone formation. The contributions to total VOCs (alkanes, alkenes, alkynes, aromatics, and carbonyl compounds) OFP at the MY, SN, ZY, YA, and LS sites ranged from 19.5% to 48.6%. Formaldehyde and acetaldehyde were identified as the most reactive species in the atmosphere, surpassing other carbonyl compounds in reactivity due to their higher concentrations and inherent reactivity, especially formaldehyde. However, acetone exhibited high inertness and a prolonged atmospheric lifetime, leading to its accumulation in ambient air with concentrations higher than other carbonyl compounds except for formaldehyde and acetaldehyde. Thus, despite its elevated concentration, acetone's reactivity remained relatively low.
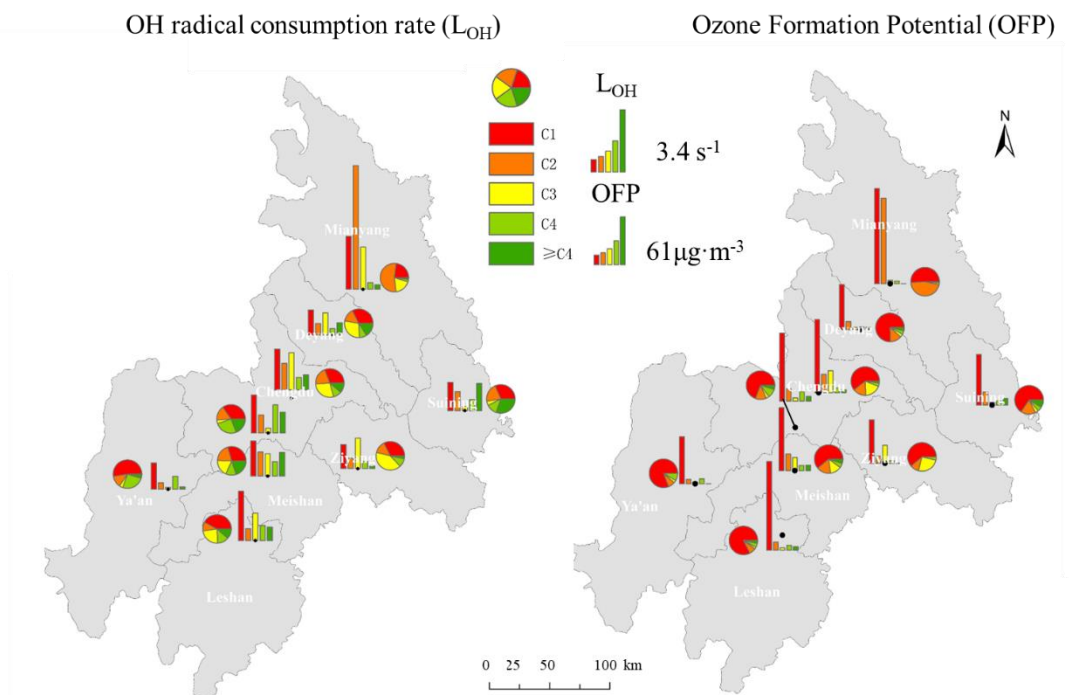
Figure 5. L_{OH} and OFP of carbonyl compounds at each site in the CPUA during the observation

591   period

3.5 Sensitivity analysis of ozone formation based on formaldehyde to NO₂ ratio (FNR)

593   The change of O₃ formation sensitivity of each site in the CPUA during the

594   observation period is shown in Fig.6. As can be seen from the Fig. 6, most sites remain

595   in the VOCs-limited regime during the cleaning period and EP1 to EP3. Economically

596   developed city such as Chengdu, Meishan, with high levels of formaldehyde and NO_2,

597   remain in the VOCs-limited regime. Ya'an as a city with the lowest GDP ranking in the

598   CPUA, with low levels of formaldehyde and NO_2, remain in the transitional regime.

599
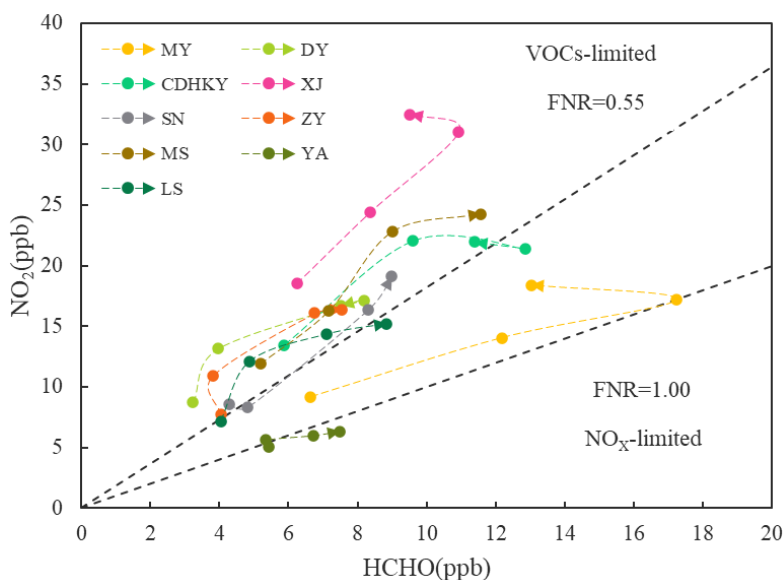
Figure 6. The change of O₃ formation sensitivity of each site in the CPUA during the observation

601   period. The arrows represent time step from clean period to EP1 to EP2 to EP3.

602   The daily variation of O₃ formation sensitivity and ozone concentration at each

603   site in the CPUA during the observation period is shown in Fig. S4. The mean FNR of

604   each site ranged from 0.48 to 1.29 during the observation period. The FNRs were lower

605   than 0.55±0.16 at XJ, DY, ZY, CDHKY, and MS, and higher than 1.0 at LS, SN, YA

606   and MY. At the same time, the mean ozone concentration at each site was between 138

607   and 192 $\mu g \cdot m^{-3}$. The mean ozone concentration in XJ, DY, CDHKY and MS was 166-

608   192 $\mu g \cdot m^{-3}$, it was 150-164 $\mu g \cdot m^{-3}$ in LS, SN, YA and MY. Therefore, it could be seen

609   that most of the sites with high mean ozone concentrations during the observation

period, like CDHKY, XJ, MS and Deyan sites, were in the VOCs-limited regime, and most of the stations with low mean ozone concentrations during the observation period such as YA, SN, MY and LS were in the transitional regime. It was worth noting that the mean ozone concentration at ZY site (only 138 μg·m^{-3}) during the observation period was much lower than that of other sites, but most of the ZY site was in VOCs-limited regime, which was mainly related to the low concentration of formaldehyde. In addition, the FNR value of the MY site was also relatively high, which was mainly caused by the high concentration of formaldehyde.

Based on the ratio of formaldehyde to NO$_2$ mixing ratio, most sites remain in the VOCs-limited regime during the observation period. And the sites with heavy ozone pollution were in the VOCs-limited regime, and the sites with light ozone pollution were in the transitional regime. Photochemical reactivity (L_{OH} and OFP) analysis showed that formaldehyde and acetaldehyde contributed significantly to the enhancement of atmospheric oxidation and ozone formation potential. Therefore, when heavy ozone pollution occurs in the CPUA, special attention should be paid to the control of VOCs, especially formaldehyde and acetaldehyde in carbonyl compounds, under the coordinated control of NOx and VOCs. Overall, this study reveals the important contribution of carbonyl compounds to ozone pollution in the CPUA, and provides scientific support for the establishment of ozone pollution prevention and control measures.

3.6 Source Analysis of carbonyl compounds

3.6.1 Quantitative source analysis of key carbonyl compounds

The table S7 provides a summary of the background and primary emissions concentrations of formaldehyde, acetaldehyde, and acetone at nine sites across the eight cities of the CPUA, along with the proportion of secondary formation contributing to their concentrations. Background concentrations and primary emissions of formaldehyde, acetaldehyde, and acetone ranged from 50% to 80%, 46% to 83%, and

45% to 78%, respectively. Secondary formation accounted for 20% to 50%, 17% to 54%, and 22% to 55% of their concentrations, respectively. Notably, in SN and YA, the secondary formation of formaldehyde contributed half of the observed concentration, indicating it as the predominant source, while acetaldehyde's secondary formation also prevailed in these sites. Conversely, acetone, with lower reactivity, primarily originated from background concentrations and primary emissions at other sites except YA. Moreover, background concentrations and primary emissions were identified as the main contributors to carbonyl compounds in XJ and LS.

Fig.7 illustrates the secondary formation concentrations of formaldehyde, acetaldehyde, and acetone at each site in the CPUA under both clean and polluted conditions. Under polluted conditions, the secondary concentrations of formaldehyde, acetaldehyde, and acetone exceeded those in clean conditions by 58.8%, 54.6%, and 57.6%, respectively. The most significant increases in secondary concentrations were observed at the SN site, while relatively smaller increases were observed at LS and XJ.
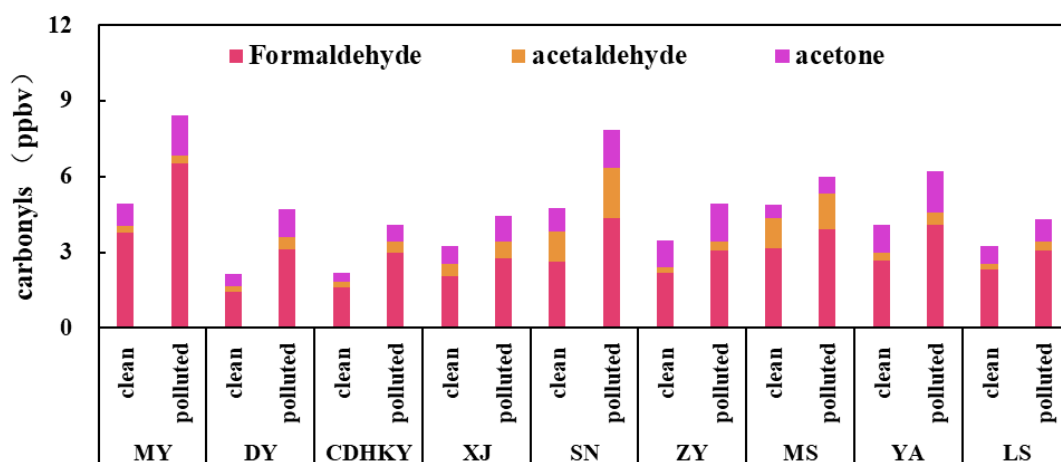
Figure 7. Concentrations of formaldehyde, acetaldehyde and acetone in secondary formation under different pollution conditions at each site in the CPUA during the observation period

3.6.2 Exploration of secondary formation mechanism of key carbonyl compounds

In this study, we utilized VOC data collected on August 11, 12, and 16, when all eight cities in the CPUA were experiencing mild to severe ozone pollution. We calculated the Relative Incremental Reactivity (RIR) of formaldehyde, acetaldehyde,

658   and acetone at the MY, SN, ZY, YA, and LS sites on these days. The OBM analysis

659   allowed us to assess the impact of anthropogenic VOCs (alkanes, alkenes, alkynes,

660   aromatics) and biogenic VOCs (e.g., isoprene) on carbonyl compound formation in the

661   context of regional ozone pollution events (Fig.8). Overall, the sensitivities of different

662   anthropogenic source and plant source VOCs to formaldehyde, acetaldehyde and

663   acetone was consistent among sites. For formaldehyde, reducing alkenes in

664   anthropogenic source VOCs and plant VOCs was the most effective way to control

665   formaldehyde concentration, while reducing alkenes in anthropogenic source VOCs

666   was also beneficial to reduce the formation of acetaldehyde. For acetone with low

667   reactivity, the alkanes in anthropogenic source VOCs were the most sensitive to the

668   formation of acetone, followed by alkenes and BVOCs. Only the RIR value of alkanes

669   were greater than zero, and the RIR values of both alkenes and BVOCs were less than

670   zero, indicating that reducing alkanes could reduce the formation of acetone, while

671   reducing alkenes and BVOCs was not conducive to acetone concentration control.
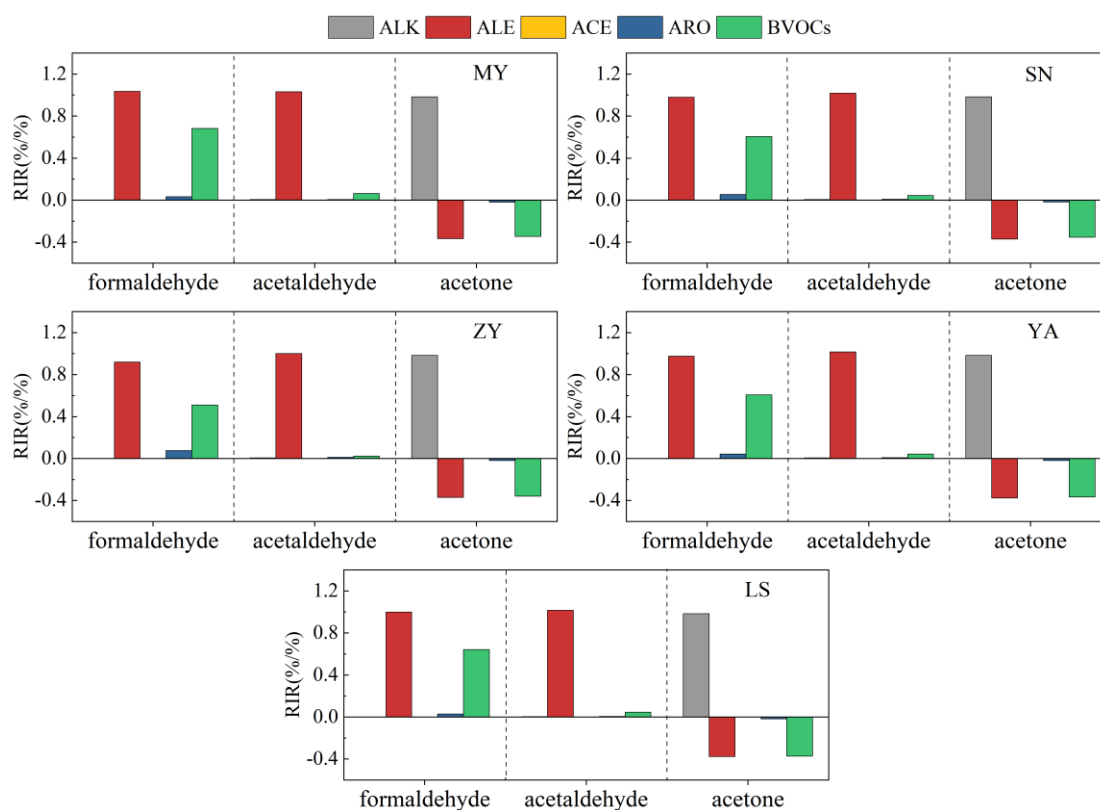

672

673   **Figure 8.** Mean RIRs of formaldehyde, acetaldehyde and acetone to different anthropogenic

674   source VOCs (alkanes (ALK), alkenes (ALE), alkynes(ACE), aromatics (ARO))and biogenic

675   VOCs (BVOCs)at MY, SN, ZY, YA and LS sites on August 11th, 12th and 16th.

3.6.3 Influence of regional transportation contribution

676

677   The TrajStat trajectory model was used to calculate and cluster the 24-hour

678   backward trajectories of air quality at the sampling sites. The backward trajectory

679   during sampling is shown in Fig.S5. During the observation period, the pollution of

680   carbonyl compounds in the cities of the CPUA was affected by the mutual transport

681   among cities in Sichuan Province, especially along the MY-DY-CDHKY route. In

682   addition, the surrounding provinces and cities of Sichuan Province (Gansu and

683   Chongqing) also contributed to the carbonyl compounds of the CPUA.

684   The potential sources of carbonyl compounds at different pollution stages at the

685   CDHKY during the observation period are shown in Fig. 9. It can be seen from the

686   figure that there are differences in the potential sources of carbonyl compounds among

687   different pollution stages at the CDHKY site. The concentration of local carbonyl

688   compounds in CDHKY was high during the early observation period and EP1, which

689   existed local sources, and was also affected by the northern airflow, and carbonyl

690   compounds was also affected by the transport from MY, DY and other northern regions.

691   Under the effect of the continuous northern airflow, the local source emissions

692   decreased during EP1, and the potential source of carbonyl compounds changed to from

693   the junction between CDHKY and ZY. During EP3, under the combined influence of

694   the western airflow, the contribution of transport from SN and ZY to carbonyl

695   compounds increased, while emissions from local sources also increased.
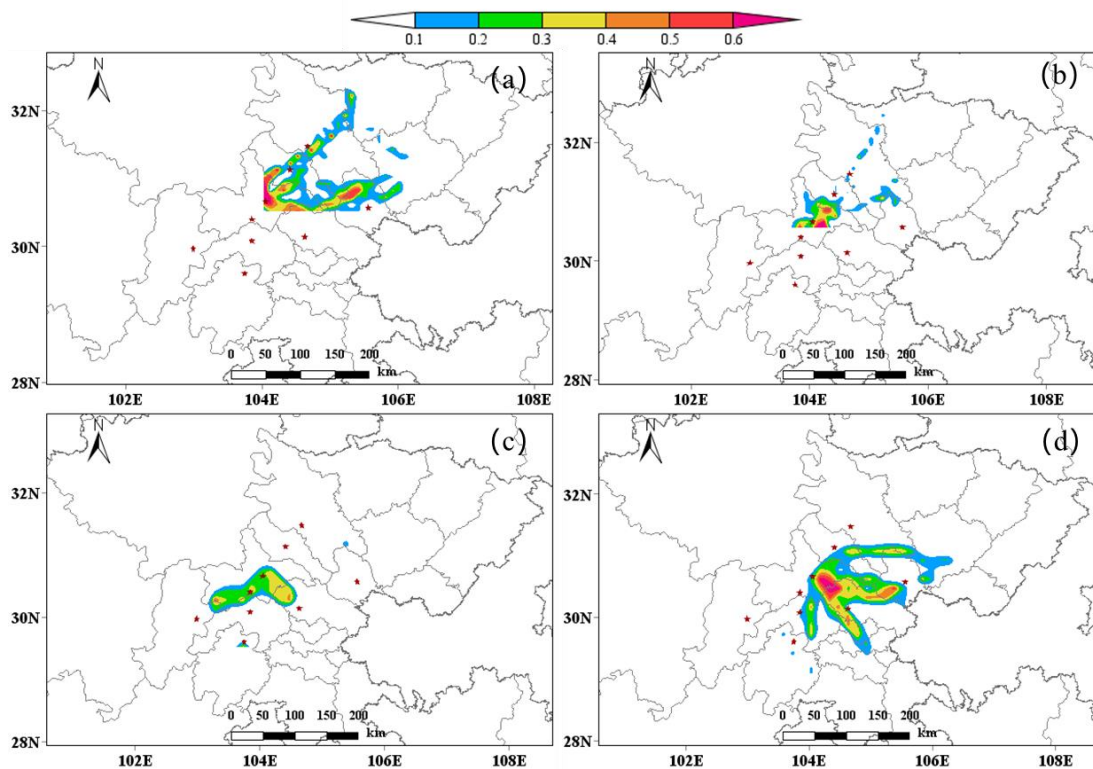
Figure 9. Analysis of potential sources of carbonyl compounds at different periods at the CDHKY site during the observation period (a) August 4th-6th (b) August 7th-9th (c) August 10th-13th (d) August 15th-18th

4. Conclusions

During a comprehensive atmospheric observation campaign conducted at nine sites across the CPUA from August 4th to 18th, 2019, three regional heavy ozone pollution episodes(EP1 to EP3) were observed. This study extensively examines the concentration variations, atmospheric chemical reactivity, and sources of carbonyls during this period. The average total concentrations of 15 carbonyl compounds across the nine sites within eight cities of the CPUA were measured at 17.4 ± 5.3 ppb. Spatial analysis indicated that areas with higher carbonyl concentrations were concentrated around Chengdu, extending both north and south. Notably, regions with elevated carbonyl compound concentrations also tended to experience more severe ozone pollution. Formaldehyde (36.4%-64.3%), acetone (12.4%-28.1%), and acetaldehyde (8.2%-47.3%) constituted the predominant species by volume concentration. Chengdu

31

712 exhibited FAT concentrations surpassing national and international levels, indicating

713 heightened levels compared to other regions.

714 Compared to clean days, carbonyl compound concentrations were significantly

715 higher on ozone pollution days, with increases ranging from 22.8% to 66.2%. Between

716 19.5% and 48.6% of the total volatile organic compound (VOC) ozone formation

717 potential (OFP) was attributed to the 15 carbonyl compounds, highlighting their

718 substantial contribution to ozone formation, particularly formaldehyde and

719 acetaldehyde. While primary emissions are the main sources of these compounds,

720 secondary formation processes contributed over 30% on average to the concentrations

721 of formaldehyde, acetaldehyde, and acetone. Under ozone pollution conditions, the

722 secondary formation concentrations of these three compounds were notably higher than

723 on clean days, with increases of 58.8%, 54.6%, and 57.6%, respectively, emphasizing

724 the critical role of secondary processes in exacerbating regional ozone pollution. OBM

725 modeling revealed that formaldehyde and acetaldehyde primarily originated from the

726 secondary formation of alkenes and BVOCs, while acetone mainly stemmed from the

727 secondary formation of alkanes. These findings highlight that while the concentration

728 of carbonyl compounds is important, their significant impact on ozone formation is

729 primarily driven by secondary chemistry. Specifically, the secondary formation of these

730 compounds from alkenes and biogenic BVOCs plays a key role in this process.

731 Ground-level observations of the formaldehyde to NO_2 ratio (FNR) were utilized

732 to assess the sensitivity of ground-level ozone formation. Analysis of FNR revealed that

733 sites experiencing heavy ozone pollution exhibited lower FNRs, indicating a VOCs-

734 limited regime, while sites with lighter ozone pollution were categorized into a

735 transitional regime. Furthermore, it is recommended to establish a scientific control

736 mechanism for both NOx and VOCs, with special attention to formaldehyde,

737 acetaldehyde, and acetone, and their alkenes precursors. Additionally, considering the

738 regional nature of pollution, this study suggests that carbonyl compound pollution is

739 influenced by mutual transport among cities within the CPUA, notably along the MY-

DY-CDHKY route. Establishing a collaborative prevention and control mechanism among cities within the CPUA and neighboring provinces and cities is crucial to effectively address carbonyl compounds and ozone pollution in the region in the future.

Data availability. Observational data including meteorological parameters and air pollutants used in this study are available from the corresponding authors upon request (lihong@craes.org.cn).

Author contributions. Hong Li and Jiemeng Bao designed this study. Xin Zhang, Zhenhai Wu, Jiemeng Bao, Li Zhou, Qinwen Tan, and Fumo Yang coordinated the selection of field observation sites, including locations for both VOCs and carbonyls grid sampling. Qinwen Tan and Hefan Liu supported the collection of carbonyls at one site. Zhenhai Wu and Xin Zhang assisted in carbonyls sampling; Xin Zhang and Yunfeng Li assisted in carbonyls sample analysis and data collection. Li Zhou and Hefan Liu organized the analysis of VOCs measurements. Jun Qian, Junhui Chen, and Liqun Deng provided support in project funding application. Jiemeng Bao performed the data analysis and wrote the paper with contributions from all co-authors; Hong Li reviewed the paper, provided comments and finalized it.

Competing interests. The contact author has declared that none of the authors has any competing interests.

781

782 **References**

783 Altshuller, A. P. (1993). Atmospheric chemistry of VOCs and NOx: Implications for
784   ozone formation. *Environmental Science & Technology*, 27(6), 1104–1117.
785   doi:10.1021/es00043a001

786 Atkinson, R., Arey, J., 2003. Atmospheric Degradation of Volatile Organic Compounds.
787   Chem. Rev. 103, 4605–4638. https://doi.org/10.1021/cr0206420

788 Bao, J., Li, H., Wu, Z., Zhang, X., Zhang, H., Li, Y., Qian, J., Chen, J., Deng, L., 2022.
789   Atmospheric carbonyls in a heavy ozone pollution episode at a metropolis in
790   Southwest China: Characteristics, health risk assessment, sources analysis.
791   Journal of Environmental Sciences 113, 40–54.
792   https://doi.org/10.1016/j.jes.2021.05.029

793 Cardelino, C., Chameides, W., 1995. An observation-based model for analyzing ozone
794   precursor relationships in the urban atmosphere. J. Air Waste Manage. Assoc.
795   45, 161–180.

796 Coggon, M. M., Veres, P. R., Yuan, B., et al. (2019). Emissions of organic carbonyl
797   compounds from biomass burning: A global source of reactive carbon to the
798   atmosphere. *Environmental Science & Technology*, 53(20), 11401–11412.

799 da Silva, D.B.N., Martins, E.M., Corrêa, S.M., 2016. Role of carbonyls and aromatics
800   in the formation of tropospheric ozone in Rio de Janeiro, Brazil. Environ Monit
801   Assess 188, 289. https://doi.org/10.1007/s10661-016-5278-3

802   Duan, J., Guo, S., Tan, J., Wang, S., Chai, F., 2012. Characteristics of atmospheric
803   carbonyls during haze days in Beijing, China. Atmospheric Research 114–115,
804   17–27. https://doi.org/10.1016/j.atmosres.2012.05.010

805   Duan, J., Tan, J., Yang, L., Wu, S., Hao, J., 2008. Concentration, sources and ozone
806   formation potential of volatile organic compounds (VOCs) during ozone
807   episode in Beijing. Atmospheric Research 88, 25–35.
808   https://doi.org/10.1016/j.atmosres.2007.09.004

809   Fu, T.-M., Jacob, D.J., Wittrock, F., Burrows, J.P., Vrekoussis, M., Henze, D.K., 2008.
810   Global budgets of atmospheric glyoxal and methylglyoxal, and implications for
811   formation of secondary organic aerosols. Journal of Geophysical Research:
812   Atmospheres 113. https://doi.org/10.1029/2007JD009505

813   Fuchs, H., Tan, Z., Lu, K., Bohn, B., Broch, S., Brown, S.S., Dong, H., Gomm, S.,
814   Häseler, R., He, L., Hofzumahaus, A., Holland, F., Li, X., Liu, Y., Lu, S., Min,
815   K.-E., Rohrer, F., Shao, M., Wang, B., Wang, M., Wu, Y., Zeng, L., Zhang,
816   Yinson, Wahner, A., Zhang, Yuanhang, 2017. OH reactivity at a rural site
817   (Wangdu) in the North China Plain: contributions from OH reactants and
818   experimental OH budget. Atmospheric Chemistry and Physics 17, 645–661.
819   https://doi.org/10.5194/acp-17-645-2017

820   Grosjean, D., & Seinfeld, J. H. (1989). Parameterization of the formation potential of
821   secondary organic aerosols. *Atmospheric Environment*, 23(8), 1733–1747.
822   doi:10.1016/0004-6981(89)90058-9

823   Guo, H., Wang, T., Simpson, I.J., Blake, D.R., Yu, X.M., Kwok, Y.H., Li, Y.S., 2004.
824   Source contributions to ambient VOCs and CO at a rural site in eastern China.
825   Atmospheric Environment 38, 4551–4560.
826   https://doi.org/10.1016/j.atmosenv.2004.05.004

827   Hallquist, M., Wenger, J. C., Baltensperger, U., et al. (2009). The formation, properties,
828   and impact of secondary organic aerosol: Current and emerging issues.
829   *Atmospheric Chemistry and Physics*, 9, 5155–5236. doi:10.5194/acp-9-5155-
830   2009

831   Ho, K.F., Ho, S.S.H., Huang, R.-J., Dai, W.T., Cao, J.J., Tian, L., Deng, W.J., 2015.
832   Spatiotemporal distribution of carbonyl compounds in China. Environmental
833   Pollution 197, 316–324. https://doi.org/10.1016/j.envpol.2014.11.014

834   Hong, Q., Zhu, L., Xing, C., Hu, Q., Lin, H., Zhang, C., Zhao, C., Liu, T., Su, W., Liu,
835   C., 2022. Inferring vertical variability and diurnal evolution of O3 formation
836   sensitivity based on the vertical distribution of summertime HCHO and NO2 in
837   Guangzhou, China. Science of The Total Environment 827, 154045.
838   https://doi.org/10.1016/j.scitotenv.2022.154045

839   Hu, J., Wang, P., Ying, Q., Zhang, H., Chen, J., Ge, X., Li, X., Jiang, J., Wang, S., Zhang,
840   J., Zhao, Y., Zhang, Y., 2017. Modeling biogenic and anthropogenic secondary
841   organic aerosol in China. Atmospheric Chemistry and Physics 17, 77–92.
842   https://doi.org/10.5194/acp-17-77-2017

843   Jiang, Z., Grosselin, B., Daële, V., Mellouki, A., Mu, Y., 2016. Seasonal, diurnal and

844 nocturnal variations of carbonyl compounds in the semi-urban environment of
845 Orléans, France. Journal of Environmental Sciences, Changing Complexity of
846 Air Pollution 40, 84–91. https://doi.org/10.1016/j.jes.2015.11.016

847 Kanjanasiranont, N., Prueksasit, T., Morknoy, D., Tunsaringkarn, T., Sematong, S.,
848 Siriwong, W., Zapaung, K., Rungsiyothin, A., 2016a. Determination of ambient
849 air concentrations and personal exposure risk levels of outdoor workers to
850 carbonyl compounds and BTEX in the inner city of Bangkok, Thailand.
851 Atmospheric Pollution Research 7, 268–277.
852 https://doi.org/10.1016/j.apr.2015.10.008

853 Kanjanasiranont, N., Prueksasit, T., Morknoy, D., Tunsaringkarn, T., Sematong, S.,
854 Siriwong, W., Zapaung, K., Rungsiyothin, A., 2016b. Determination of ambient
855 air concentrations and personal exposure risk levels of outdoor workers to
856 carbonyl compounds and BTEX in the inner city of Bangkok, Thailand.
857 Atmospheric Pollution Research 7, 268–277.
858 https://doi.org/10.1016/j.apr.2015.10.008

859 Li, N., Fu, T.-M., Cao, J., Lee, S., Huang, X.-F., He, L.-Y., Ho, K.-F., Fu, J.S., Lam, Y.-
860 F., 2013. Sources of secondary organic aerosols in the Pearl River Delta region
861 in fall: Contributions from the aqueous reactive uptake of dicarbonyls.
862 Atmospheric Environment, Improving Regional Air Quality over the Pearl
863 River Delta and Hong Kong: from Science to Policy 76, 200–207.
864 https://doi.org/10.1016/j.atmosenv.2012.12.005

865 Li, Y., Shao, M., Lu, S., Chang, C.-C., Dasgupta, P.K., 2010. Variations and sources of
866 ambient formaldehyde for the 2008 Beijing Olympic games. Atmospheric
867 Environment 44, 2632–2639. https://doi.org/10.1016/j.atmosenv.2010.03.045

868 Ling, Z.H., Zhao, J., Fan, S.J., Wang, X.M., 2017. Sources of formaldehyde and their
869 contributions to photochemical O3 formation at an urban site in the Pearl River
870 Delta, southern China. Chemosphere 168, 1293–1301.
871 https://doi.org/10.1016/j.chemosphere.2016.11.140

872 Liu, J., Li, X., Tan, Z., Wang, W., Yang, Y., Zhu, Y., Yang, S., Song, M., Chen, S., Wang,
873 H., Lu, K., Zeng, L., Zhang, Y., 2021. Assessing the Ratios of Formaldehyde
874 and Glyoxal to NO2 as Indicators of O3–NOx–VOC Sensitivity. Environ. Sci.
875 Technol. 55, 10935–10945. https://doi.org/10.1021/acs.est.0c07506

876 Lou, S., Holland, F., Rohrer, F., Lu, K., Bohn, B., Brauers, T., Chang, C.C., Fuchs, H.,
877 Häseler, R., Kita, K., Kondo, Y., Li, X., Shao, M., Zeng, L., Wahner, A., Zhang,
878 Y., Wang, W., Hofzumahaus, A., 2010. Atmospheric OH reactivities in the Pearl
879 River Delta – China in summer 2006: measurement and model results.
880 Atmospheric Chemistry and Physics 10, 11243–11260.
881 https://doi.org/10.5194/acp-10-11243-2010

882 Luecken, D.J., Hutzell, W.T., Strum, M.L., Pouliot, G.A., 2012. Regional sources of
883 atmospheric formaldehyde and acetaldehyde, and implications for atmospheric
884 modeling. Atmospheric Environment 47, 477–490.
885 https://doi.org/10.1016/j.atmosenv.2011.10.005

Lui, K.H., Ho, S.S.H., Louie, P.K.K., Chan, C.S., Lee, S.C., Hu, D., Chan, P.W., Lee, J.C.W., Ho, K.F., 2017. Seasonal behavior of carbonyls and source characterization of formaldehyde (HCHO) in ambient air. Atmospheric Environment 152, 51–60. https://doi.org/10.1016/j.atmosenv.2016.12.004

Monks, P. S., Archibald, A. T., Colette, A., Cooper, O., Coyle, M., Derwent, R., ... & Williams, M. L. (2015). Tropospheric ozone and its precursors from the urban to the global scale from air quality to short-lived climate forcer. *Atmospheric Chemistry and Physics*, 15(15), 8889-8973.

Murillo, J.H., Marín, J.F.R., Román, S.R., 2012. Determination of carbonyls and their sources in three sites of the metropolitan area of Costa Rica, Central America. Environ Monit Assess 184, 53–61. https://doi.org/10.1007/s10661-011-1946-5

Pang, X., Mu, Y., 2006. Seasonal and diurnal variations of carbonyl compounds in Beijing ambient air. Atmospheric Environment 40, 6313–6320. https://doi.org/10.1016/j.atmosenv.2006.05.044

Rao, Z., Chen, Z., Liang, H., Huang, L., Huang, D., 2016. Carbonyl compounds over urban Beijing: Concentrations on haze and non-haze days and effects on radical chemistry. Atmospheric Environment, Air Pollution in the Beijing – Tianjin – Hebei (BTH) region, China 124, 207–216. https://doi.org/10.1016/j.atmosenv.2015.06.050

Sahu, L. K., & Saxena, P. (2015). High time-resolved volatile organic compounds measurements at an urban location in India: Sources, variability, and role in ozone formation. *Environmental Science and Pollution Research*, 22(5), 3975-3986.

Schroeder, J.R., Crawford, J.H., Fried, A., Walega, J., Weinheimer, A., Wisthaler, A., Müller, M., Mikoviny, T., Chen, G., Shook, M., Blake, D.R., Tonnesen, G.S., 2017. New insights into the column CH2O/NO2 ratio as an indicator of near-surface ozone sensitivity. Journal of Geophysical Research: Atmospheres 122, 8885–8907. https://doi.org/10.1002/2017JD026781

Shao, M., Lu, S., Liu, Y., Xie, X., Chang, C., Huang, S., Chen, Z., 2009. Volatile organic compounds measured in summer in Beijing and their role in ground-level ozone formation. Journal of Geophysical Research: Atmospheres 114. https://doi.org/10.1029/2008JD010863

Shen, X., Zhao, Y., Chen, Z., Huang, D., 2013. Heterogeneous reactions of volatile organic compounds in the atmosphere. Atmospheric Environment 68, 297–314. https://doi.org/10.1016/j.atmosenv.2012.11.027

Tan, Z., Lu, K., Jiang, M., Su, R., Dong, H., Zeng, L., Xie, S., Tan, Q., Zhang, Y., 2018. Exploring ozone pollution in Chengdu, southwestern China: A case study from radical chemistry to O3-VOC-NOx sensitivity. Science of The Total Environment 636, 775–786. https://doi.org/10.1016/j.scitotenv.2018.04.286

Tonnesen, G.S., Dennis, R.L., 2000. Analysis of radical propagation efficiency to assess ozone sensitivity to hydrocarbons and NO x : 2. Long-lived species as indicators of ozone concentration sensitivity. Journal of Geophysical Research:

Atmospheres 105, 9227–9241. https://doi.org/10.1029/1999JD900372

Vermeuel, M.P., Novak, G.A., Alwe, H.D., Hughes, D.D., Kaleel, R., Dickens, A.F., Kenski, D., Czarnetzki, A.C., Stone, E.A., Stanier, C.O., Pierce, R.B., Millet, D.B., Bertram, T.H., 2019. Sensitivity of Ozone Production to NOx and VOC Along the Lake Michigan Coastline. Journal of Geophysical Research: Atmospheres 124, 10989–11006. https://doi.org/10.1029/2019JD030842

Wang, C., Huang, X.-F., Han, Y., Zhu, B., He, L.-Y., 2017. Sources and Potential Photochemical Roles of Formaldehyde in an Urban Atmosphere in South China. Journal of Geophysical Research: Atmospheres 122, 11,934-11,947. https://doi.org/10.1002/2017JD027266

Wang, Y., Guo, H., Zou, S., Lyu, X., Ling, Z., Cheng, H., Zeren, Y., 2018. Surface O3 photochemistry over the South China Sea: Application of a near-explicit chemical mechanism box model. Environmental Pollution 234, 155–166. https://doi.org/10.1016/j.envpol.2017.11.001

Wang, Y., Wang, H., Zhang, X., et al. (2020). Formation of secondary organic aerosols from carbonyl compounds: Insights from field observations and simulations. *Atmospheric Chemistry and Physics*, 20, 6177–6189.

Xue, L., Gu, R., Wang, T., Wang, X., Saunders, S., Blake, D., Louie, P.K.K., Luk, C.W.Y., Simpson, I., Xu, Z., Wang, Z., Gao, Y., Lee, S., Mellouki, A., Wang, W., 2016. Oxidative capacity and radical chemistry in the polluted atmosphere of Hong Kong and Pearl River Delta region: analysis of a severe photochemical smog episode. Atmospheric Chemistry and Physics 16, 9891–9903. https://doi.org/10.5194/acp-16-9891-2016

Xue, L.K., Wang, T., Gao, J., Ding, A.J., Zhou, X.H., Blake, D.R., Wang, X.F., Saunders, S.M., Fan, S.J., Zuo, H.C., Zhang, Q.Z., Wang, W.X., 2014. Ground-level ozone in four Chinese cities: precursors, regional transport and heterogeneous processes. Atmospheric Chemistry and Physics 14, 13175–13188. https://doi.org/10.5194/acp-14-13175-2014

Xue, L.K., Wang, T., Guo, H., Blake, D.R., Tang, J., Zhang, X.C., Saunders, S.M., Wang, W.X., 2013. Sources and photochemistry of volatile organic compounds in the remote atmosphere of western China: results from the Mt. Waliguan Observatory. Atmospheric Chemistry and Physics 13, 8551–8567. https://doi.org/10.5194/acp-13-8551-2013

Xue, L., Wang, T., Louie, P. K. K., Luk, C. W. Y., Blake, D. R., Gao, J., & Lee, S. H. (2013). Increasing external effects negate local efforts to control ozone air pollution: A case study of Hong Kong and implications for other Chinese cities. Environmental Science & Technology, 47(17), 10299-10305.

Yang, X., Xue, L., Wang, T., Wang, X., Gao, J., Lee, S., Blake, D.R., Chai, F., Wang, W., 2018. Observations and Explicit Modeling of Summertime Carbonyl Formation in Beijing: Identification of Key Precursor Species and Their Impact on Atmospheric Oxidation Chemistry. Journal of Geophysical Research: Atmospheres 123, 1426–1440. https://doi.org/10.1002/2017JD027403

Yang, X., Xue, L., Yao, L., Li, Q., Wen, L., Zhu, Y., Chen, T., Wang, X., Yang, L., Wang, T., Lee, S., Chen, J., Wang, W., 2017. Carbonyl compounds at Mount Tai in the North China Plain: Characteristics, sources, and effects on ozone formation. Atmospheric Research 196, 53–61. https://doi.org/10.1016/j.atmosres.2017.06.005

Ye, Z., Xie, S., Wu, Y., et al. (2021). Characterization of carbonyl compounds and their contributions to ozone and secondary organic aerosol formation in a megacity. *Environmental Science & Technology*, 55(14), 9465–9474.

Yuan, B., Chen, W., Shao, M., Wang, M., Lu, S., Wang, Bin, Liu, Y., Chang, C.-C., Wang, Boguang, 2012. Measurements of ambient hydrocarbons and carbonyls in the Pearl River Delta (PRD), China. Atmospheric Research, Remote Sensing of Clouds and Aerosols: Techniques and Applications - Atmospheric Research 116, 93–104. https://doi.org/10.1016/j.atmosres.2012.03.006

Zhang, X., Chen, Z.M., Zhao, Y., 2010. Laboratory simulation for the aqueous OH-oxidation of methyl vinyl ketone and methacrolein: significance to the in-cloud SOA production. Atmospheric Chemistry and Physics 10, 9551–9561. https://doi.org/10.5194/acp-10-9551-2010

Zhang, X., Wu, Z., He, Z., Zhong, X., Bi, F., Li, Y., Gao, R., Li, H., Wang, W., 2022. Spatiotemporal patterns and ozone sensitivity of gaseous carbonyls at eleven urban sites in southeastern China. Science of The Total Environment 824, 153719. https://doi.org/10.1016/j.scitotenv.2022.153719

Zhang, Y., Wang, X., Wen, S., Herrmann, H., Yang, W., Huang, X., Zhang, Z., Huang, Z., He, Q., George, C., 2016. On-road vehicle emissions of glyoxal and methylglyoxal from tunnel tests in urban Guangzhou, China. Atmospheric Environment 127, 55–60. https://doi.org/10.1016/j.atmosenv.2015.12.017

Zhang, Z., Zhang, Y., Wang, X., Lü, S., Huang, Z., Huang, X., Yang, W., Wang, Y., Zhang, Q., 2016. Spatiotemporal patterns and source implications of aromatic hydrocarbons at six rural sites across China's developed coastal regions. Journal of Geophysical Research: Atmospheres 121, 6669–6687. https://doi.org/10.1002/2016JD025115

Zhou, Z., Tan, Q., Deng, Y., Lu, C., Song, D., Zhou, X., Zhang, X., Jiang, X., 2021. Source profiles and reactivity of volatile organic compounds from anthropogenic sources of a megacity in southwest China. Science of The Total Environment 790, 148149. https://doi.org/10.1016/j.scitotenv.2021.148149